Optical Turbulence Simulations from a Numerical Weather Prediction Model in Support of Air to Air Laser Communications

Randall J. Alliss and Billy D. Felton

Northrop Grumman Information Systems/TASC
4801 Stonecroft Blvd.
Chantilly, VA 20151

Abstract

Optical turbulence (OT) acts to distort light in the atmosphere, degrading imagery from large astronomical telescopes and possibly reducing data quality of air to air laser communication links. Some of the degradation due to turbulence can be corrected by adaptive optics. However, the severity of optical turbulence, and thus the amount of correction required, is largely dependent upon the turbulence at the location of interest. Therefore, it is vital to understand the climatology of optical turbulence at such locations. In many cases, it is impractical and expensive to setup instrumentation to characterize the climatology of OT, so simulations become a less expensive and convenient alternative.

The strength of OT is characterized by the refractive index structure function Cn^2, which in turn is used to calculate atmospheric seeing parameters. While attempts have been made to characterize Cn^2 using empirical models, Cn^2 can be calculated more directly from Numerical Weather Prediction (NWP) simulations using pressure, temperature, thermal stability, vertical wind shear, turbulent Prandtl number, and turbulence kinetic energy (TKE). In this work we use the Weather Research and Forecast (WRF) NWP model to generate Cn^2 climatologies in the planetary boundary layer and free atmosphere, allowing for both point-to-point, air to air, and ground-to-space seeing estimates of the Fried Coherence length (r_o) and other seeing parameters. Simulations are performed using the Maui High Performance Computing Centers Jaw's cluster.

The WRF model is configured to run at 1km horizontal resolution over a domain covering the islands of Maui and the Big Island. The vertical resolution varies from 50 meters in the boundary layer to 500 meters in the stratosphere. The model top is 20 km. We are interested in the variations in Cn^2 and the Fried Coherence Length (r_o) between the summits of Haleakala and Mauna Loa. Six months of simulations have been performed over this area. Simulations indicate that the vast lava fields which characterize the Big Island to the shoreline have a large impact on turbulence generation. The same turbulence characteristics are also present in the simulations on the Southeastern face of Haleakala. Turbulence is greatest during the daytime when the lava fields produce tremendous heat fluxes. Good agreement is found when the WRF simulations are compared to *in situ* data taken from the Advanced Technology Solar Telescope (ATST) Site Survey Working Group at the Mees Solar Observatory on Haleakala, particularly during the middle of the day. The ATST used a solar DIMM instrument; therefore comparisons were limited to daytime. Both the WRF simulations and ATST showed r_o values bottoming out in the 3-4 cm range during daytime. Analysis of the horizontal path between Haleakala and Mauna Loa show minimum r_o dropping below 1 cm during the peak heating of the day. We are awaiting horizontal observations of Cn^2 to become available to continue the validation exercises. Results of these analyses are assisting communication engineers in developing state of the art adaptive optic designs. Detailed results of this study will be presented at the conference.

1. Introduction

With High Performance Computing (HPC) platforms becoming much more affordable and accessible, simulations of physical quantities in the atmosphere are easily performed. An excellent example of this is free space optical turbulence (OT). OT is an important atmospheric phenomenon, particularly for astronomers, because of the impact it has on seeing. Small-scale temperature and moisture fluctuations in the atmosphere result in fluctuations of the refractive index. The wave front of radiation traveling through the atmosphere changes as it encounters inhomogeneities in the refractive index, degrading optical image quality. The intensity of the turbulent fluctuations of the atmospheric refractive index is described by the refractive index structure function, C_n^2. The ability to quantify the amount of OT above an observatory and to understand its vertical distribution is vital and can impact decisions on adaptive optics design, observatory scheduling, and site selection for new observatories. Although instruments have been developed to characterize OT, they are expensive to maintain over long durations of time and the quality is limited.

Numerical simulations of OT are an attractive alternative to local observations in regions where infrastructure (i.e., electrical power) is lacking. Numerical simulations offer many advantages over direct measurements.

These advantages include a three-dimensional description of C_n^2 over regions of interest, simulations that can be performed anywhere on earth at any time, and the ability to provide forecasts of OT that could be used for observational scheduling purposes. The reliability of these types of simulations for describing the climatology of OT has recently been shown to be quite good.

Our approach to simulate OT employs a model used to predict tropospheric weather. These models are referred to by the meteorological community as Numerical Weather Prediction (NWP). NWP models are routinely used by meteorologists to predict everyday weather. However, in this application the model is modified to make simulations of C_n^2. In this paper we describe how NWP is leveraged to simulate OT and present various results along with intercomparisons to direct observations of integrated OT.

2. Technical Approach

In this study we use version 3.0 of the Weather Research and Forecasting (WRF) model developed jointly by the National Center for Atmospheric Research (NCAR) and the National Oceanic and Atmospheric Administration (NOAA) (Skamarock et al., 2008). WRF is a mesoscale NWP model developed for the prediction of weather and is routinely used by the National Weather Service and other forecasting services. The model is based on the Navier Stokes equations, which are solved numerically on a three-dimensional grid. Four basic atmospheric properties are simulated by the model from which all others variables are derived. These properties are wind, pressure, temperature, and atmospheric water vapor.

This study used the WRF model to develop a climatology of OT over the Hawaiian Islands including the summits on Maui and the Big Island. The following sections describe the model setup, modifications to the code, and derivation of OT parameters followed by results of simulations to date.

a. Model Setup

WRF is used to simulate daily meteorological conditions for the Hawaii domain for the six month period May – October 2008. The model is configured at 1-km horizontal resolution with dimensions of 273x273 grid points and 83 vertical levels. The resolution of the vertical levels is approximately 50-m resolution below 2 km above ground level (AGL), 125 m for 2–12 km AGL, and 500 m up to the model top (50 millibars). Simulations are initialized at 1200 UTC directly from the 36-km Global Forecasting System (GFS) analysis produced by the National Weather Service. Lateral boundary conditions are provided out to 27 hours by three-hourly GFS forecasts. This allows for filtering out model "spin-up" by excluding the first three simulation hours, while still capturing the full 24-hour diurnal cycle. Selected physics and diffusion options are summarized in Table 1.The model was reinitialized each day during the six month period.

Table 1. Physics and diffusion settings used in WRF model for this study

Time Integration	RK3
Time Step	2 sec
Horizontal/Vertical Advection	Fifth/Third order
Explicit Diffusion	Physical space 2D deformation, no sixth order
Boundary Layer Physics	Mellor, Yamada, Janjic (MYJ)
Surface Layer	Janjic Eta
Land Surface	Noah
Shortwave/Longwave Radiation	Dudhia/RRTM
Microphysics	WSM6
Cumulus Parameterization	None

b. Model Modifications

The minimum turbulence kinetic energy (TKE) permitted in the Mellor-Yamada-Janjic (MYJ) scheme had to be modified. The default setting gives TKE values >0.1 m^2s^{-2}, resulting in unrealistically large values of C_n^2 in the free atmosphere. Following Gerrity et al. (1994), the minimum TKE limit was changed to 10^{-5} m^2s^{-2}. The second modification involves the eddy diffusivities of heat and momentum (K_H and K_M, respectively). In the original MYJ scheme, these variables are given by

$$K_h = l_q S_H \quad , K_h = l_q S_{M,}$$

Where l is the mixing length, $q = \sqrt{2TKE}$, and $S_{H,}$ and $S_{M,}$ are functions of TKE, mixing length, buoyancy, and vertical wind shear (Mellor and Yamada, 1982). In the modified version these relationships are unchanged for neutral and unstable conditions. However, when the gradient Richardson number (Ri) > 0.01, an implementation by Walters and Miller (1999) is followed whereby K_M is adjusted according to:

$$\frac{K_H}{K_M} = \begin{cases} \dfrac{1}{7Ri,} \; for Ri \geq 1, \\ \dfrac{1}{6.873Ri + \dfrac{1}{1+6.873Ri}} \; for 0.01 < Ri \leq 1. \end{cases}$$

The $\frac{K_H}{K_M}$ equation was first proposed by Kondo et al. (1978). The Kondo equation decreases $\frac{K_H}{K_M}$ with increasing Ri, effectively increasing the TKE production by vertical wind shear. This is necessary to generate free atmospheric turbulence that is commonly associated with jet streams. Without this change the model rarely produces TKE larger than the model's minimum value, something that is considered unrealistic when compared to many global thermosonde measurements (Ruggiero, personal communication, 2008).

c. Derivation of Seeing

This study is interested in the vertical distribution of the refractive index structure function C_n^2. When turbulence is locally homogeneous and isotropic, C_n^2 is related to changes in the refractive index. Large values of C_n^2 correspond to increasing changes in the refractive index and thus greater turbulence. Tatarskii (1971) derived an alternative expression for the structure function parameter applicable for optical wavelengths:

$$C_n^2 = \left(\frac{79 * 10^{-8} P}{T^2} \right)^2 C_T^2$$

where *P* is atmospheric pressure, *T* is air temperature, and C_T^2 is the structure function parameter for temperature. C_T^2 is given by:

$$C_T^2 = a^2 \left(\frac{K_H}{K_M} \right) L_o^{\frac{4}{3}} \left(\frac{\partial \theta}{\partial Z} \right)^2$$

Where a^2 is an empirical constant, L_o is the outer length scale of turbulence (i.e., the upper bound of the inertial subrange), and $\left(\frac{\partial \theta}{\partial Z} \right)$ is the vertical gradient of potential temperature. Following Walters and Miller (1999), a^2 is set to 2.8 and calculation of the outer length scale of turbulence in the thermally stable conditions is approximated from Deardorff (1980):

$$L_o = 0.76 \sqrt{\frac{TKE}{N}}$$

where *N* is the Brunt-Vaisala frequency. In thermally unstable conditions, L_o is related to the depth of the unstable boundary layer.

In this study we also compute Fried's Coherence Length (r_o), which is a measure of phase distortion of an optical wave front by turbulence. r_o can vary rapidly over time and from one point of the sky to another. This

parameter represents the integrated effect of turbulence along a line of sight. Larger (smaller) values of r_o are indicative of less (more) turbulence and better seeing. After Fried (1965), it is calculated by integrating C_n^2 along a path, *z*:

$$r_o = \left[0.423 \left(\frac{2\Pi}{\lambda} \right)^2 \int_0^\infty C_n^2(z) dz \right]^{-3/5}$$

3. Results

Three-dimensional turbulence simulations were made over the state of Hawaii (Figure 1) once per day during the months May – October 2008. The figure indicates the terrain heights in meters above sea level. Not the three main peaks on the islands including Haleakala on Maui, and Mauna Loa and Mauna Kea on the Big Island. These islands are characterized by steeply rising volcanic mountains, ridges and ravines. The windward sides of the islands are subject to the Northeast trade winds which blow the majority of the year. These trades produce wet conditions on the windward side of the islands compared to the leeward side. Clouds are typical trapped below the trade wind boundary layer around 2km making the summits quite clear (Figure 2b).

The WRF simulations were generated at the Maui High Performance Computing Center (MHPCC) and took approximately 800 wall clock hours to complete.

Because the model output contains many terabytes of information a tool was developed to facilitate analysis of these data. This tool makes use of the Python scripting language to control data ingest and graphical user interface attributes and Matlab for data display. The tool provides a two-dimensional view of the topography over the selected domain. The tool allows the user to load any month or year of data and to quickly look at two-dimensional plots of various seeing parameters including r_o, Θ_o and the Greenwood Frequency, f_G, as a function of time of day. This allows for analysis of how the turbulence may be distributed horizontally across the domain. The user may also look at the distribution of any of these parameters for a single vertical column in the domain.

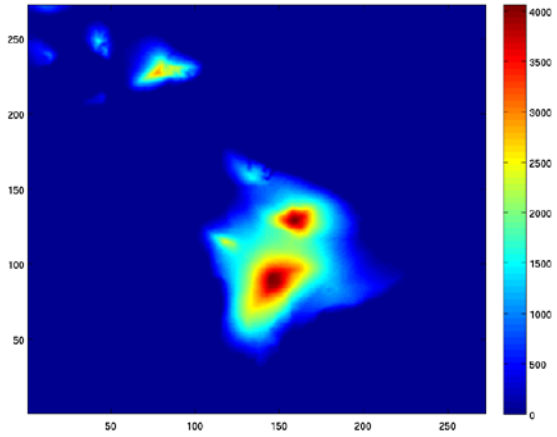

Figure 1. WRF Domain over the Hawaiian Islands. Terrain heights are in meters above sea level.

The mean r_o over the entire domain is shown in Figure 2a. The values are referenced to zenith and are valid at 500nm. The simulations indicate that the best seeing occurs just below the three summits (9-11cm) with a relative minimum in r_o at summit level (7-9cm). At first glance this may not appear reasonable. However, simulations indicate surface winds are stronger at peak level compared to elevations only 200 meters below the peaks. There appears to be a minimum in wind speed immediately to the leeward side of the peaks, particularly at Haleakala. The majority of the turbulence developed by the model is in the surface layer so this is not unreasonable. Bradley et. al 2006 reports that with the prevailing winds from the east to northeast, the air must cross over the caldera before reaching the observatories on Haleakala. This has the effect of increasing the turbulence immediately above the site. Since the WRF model was configured to have limited vertical resolution near the surface the model may be picking up on this process and over predicting the turbulence at summit level. It is also postulated that the better seeing produced in the WRF simulations below summit level are an effect of mountain blocking. We are in the process of trying to find surface observations below peak which will corroborate these findings. Figure 2b shows the mean cloud amount over the islands for the same six month period. The cloud analysis was derived from the Northrop Grumman Cloud Mask Generator (CMG). The CMG produces a pixel level cloud analysis based on the NOAA Geostationary Operational Environmental Satellite (GOES) series of satellites. Figure 2a&b shows the correlation between the occurrence of clouds and seeing conditions. Figure 3 provides a zoomed in version over Haleakala with terrain contours overlaid. Figure 3 clearly shows that the best seeing is just below summit level, however, it should be noted that it is also much cloudier (Figure 2b). The layer just below summit level on Haleakala is dominated by

the top of the trade wind boundary layer. This layer is often dominated by stratocumulus type clouds which are generally trapped below the summit level.

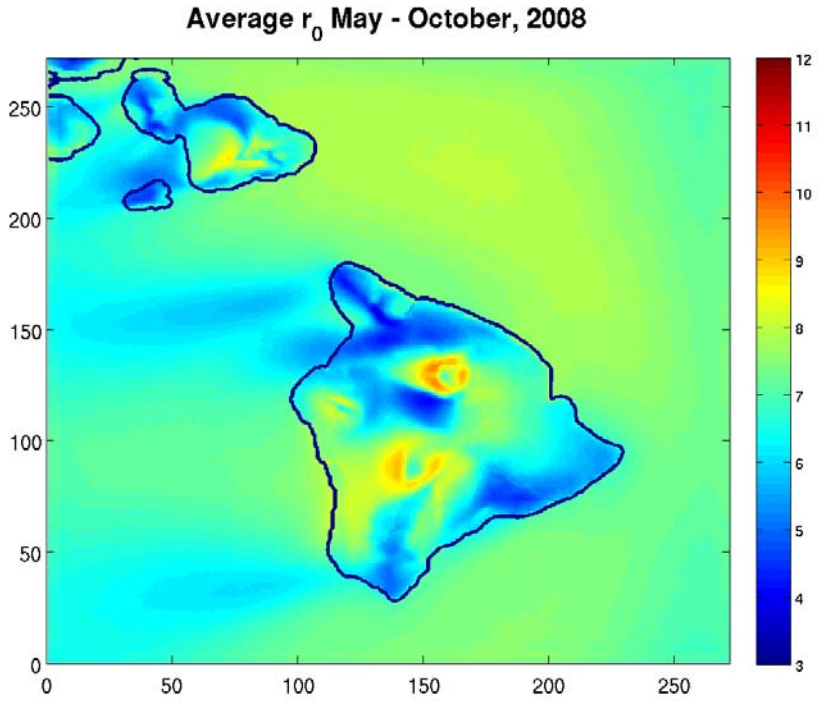

Figure 2a. Mean r0 over the Hawaiian domain for the period May – October 2008. Data is referenced to zenith and is valid at 500 nm.

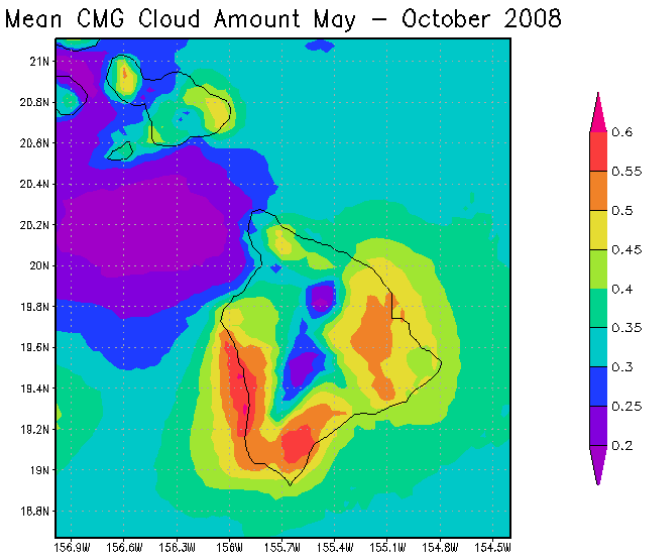

Figure 2b. The mean cloud amount derived from the GOES Cloud Mask Generator (CMG) software at Northrop Grumman for the period May – October 2008.

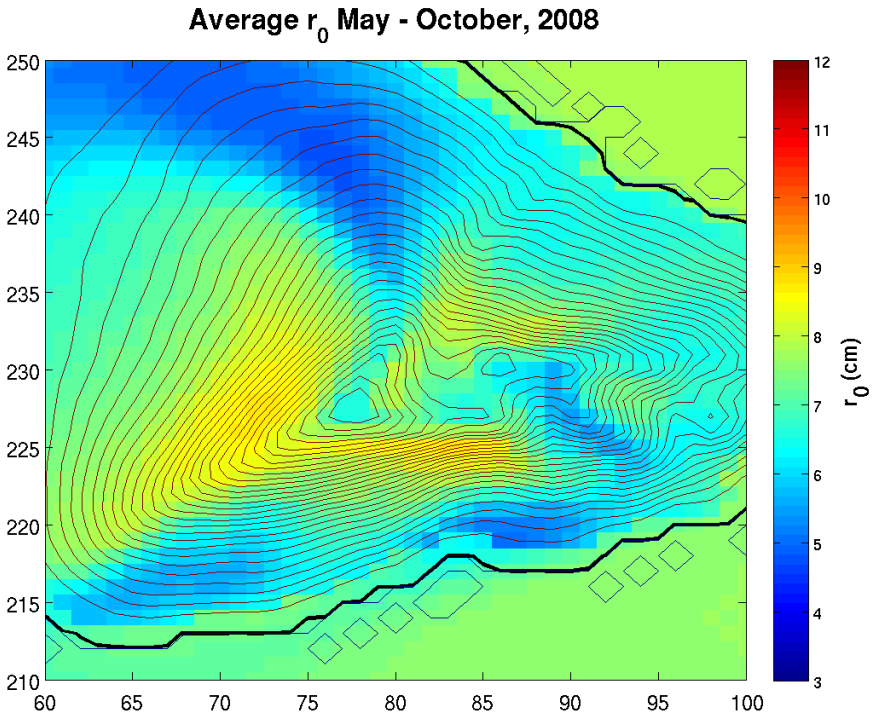

Figure 3. Mean r0 over the Maui for the period May – October 2008. Terrain lines are in 100 meter increments. Data is referenced to zenith and is valid at 500 nm.

Figures 4 shows maps of r_o at 0600 UTC (sunset), 1200 UTC (night), 1600 UTC (sunrise) and 2300 UTC (afternoon) zoomed into Haleakala. The diurnal variation is clearly evident as peak r_o (best seeing) is found at night and poorest seeing is found during the daytime. The simulations continue to show that regardless of time of day the best seeing is found just below summit level on the western and southern slopes of Haleakala. Again it is difficult to validate these simulations without observations below the summit level. Because we are interested in comparing the WRF simulations to observations we have focused our analysis on at r_o Haleakala. Figure 5 shows the diurnal variation of simulated r_o along with error bars representing plus and minus two standard deviations. As the figure indicates the data shows the classic pattern of good seeing at night and relatively poor seeing during the peak heating hours of the late afternoon. Maximum r_o are approximately 9 cm at night and 5 cm during the peak heating hours. The 2-sigma error bars are approximately 7cm at night but decrease slightly to 4 cm during daytime. The majority of the turbulence is generated in the first few hundred meters of the surface with a secondary maximum at the jet stream level. Interestingly, the data does not show the classic "neutral event" at sunrise or at sunset that has been observed (Bradley, et al., 2006). Instead the simulations show very little variation in seeing throughout the night and not a secondary maximum in r_o as reported by others. Overall the mean r_o at Haleakala as reported by WRF is 7.5cm. The calculation of r_o includes those times when clouds are present in the model. This has the effect of decreasing the seeing conditions. When removing the clouds the value of r_o increases to approximately 8.5 cm. According to other sources as reported in (Bradley, et al., 2006) mean observed r_o with various sensors at Haleakala range from 8.3 cm to 28 cm. This puts the WRF simulations on the low end of the range of reported seeing. Although, these simulations are only for a limited time of year, we believe the WRF model may be too energetic in developing turbulence because of errors in the land type modeling. This is currently being investigated. We have found a strong correlation between r_o and wind speed and wind direction. Worse seeing is correlated with wind directions from the Northeast and East as well as with higher wind speeds. The model generates a relative minimum in wind speed at the Haleakala summit compared with slightly lower elevations. This explains, partly, the poorer seeing at summit level as reported earlier.

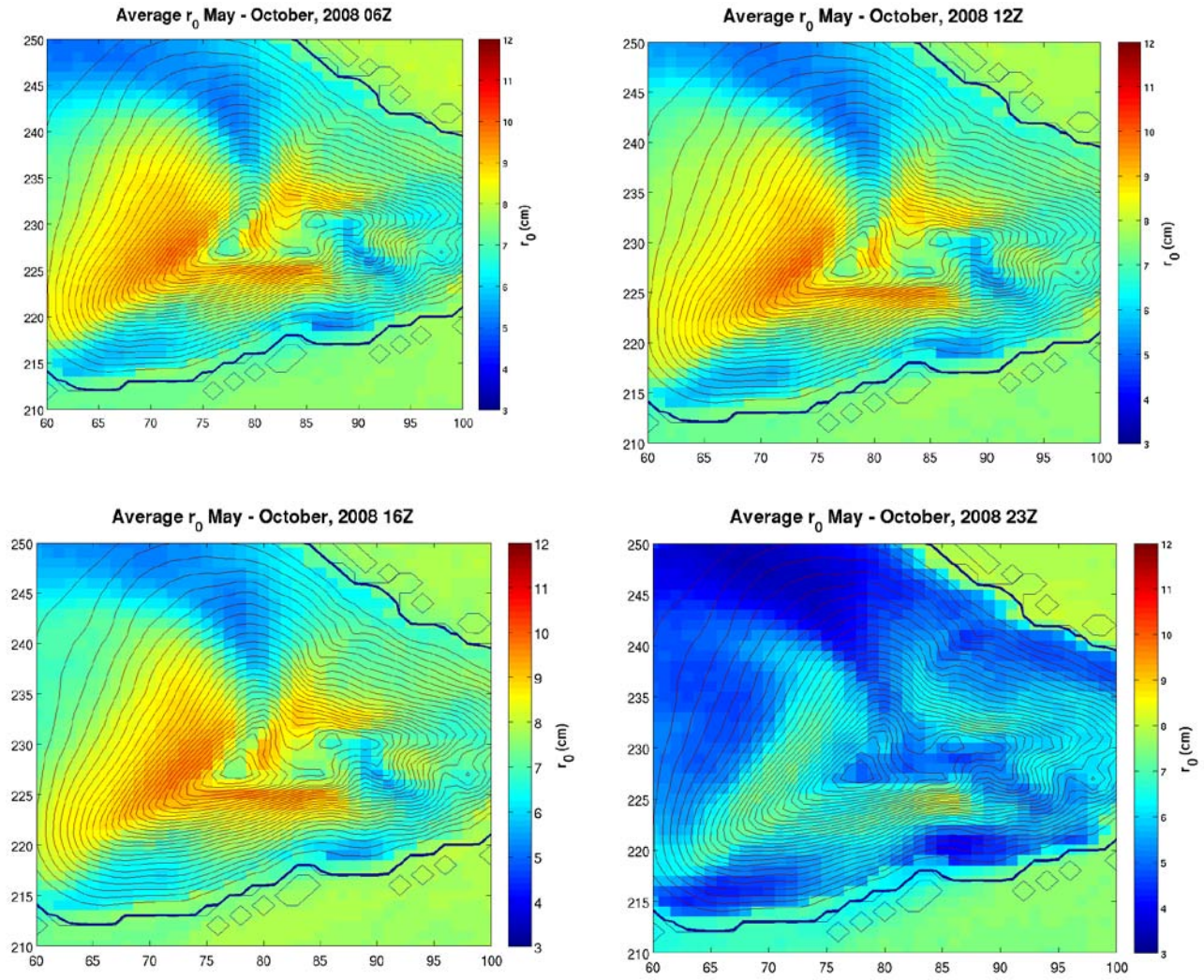

Figure 4. The diurnal variation in WRF simulated r_o for (a) 0600 UTC, (b) 1200 UTC, (c) 1600 UTC, and (d) 2300 UTC. Data is referenced to zenith and is valid at 500 nm.

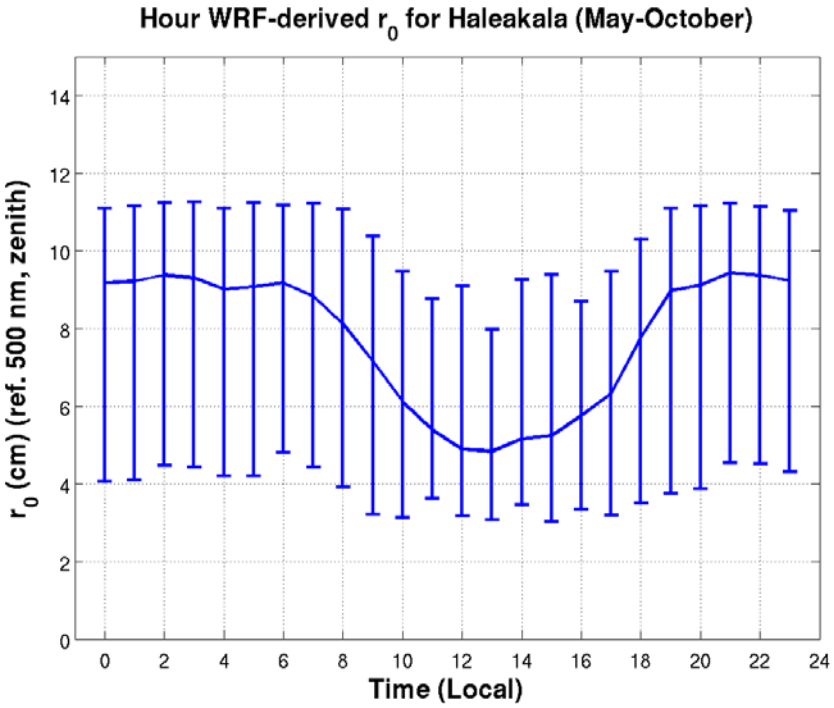

Figure 5. The diurnal variation in WRF simulated r_o at Haleakala. Data is referenced to zenith and is valid at 500 nm.

In order to conduct a validation exercise we wanted to compare the WRF simulations of r_o with *in situ* data collected over an extended time frame. Data was obtained from the Advanced Technology Solar Telescope (ATST) Site Survey Working Group at the Mees Solar Observatory on Haleakala. ATST will be the largest solar telescope in the world, with unprecedented abilities to view details of the Sun *(ATST Site Survey Working Group Final Report, 2004)*. Using adaptive optics technology, ATST will be able to provide the sharpest views ever taken of the solar surface, which will allow scientists to learn even more about the Sun and solar-terrestrial interactions. The ATST seeing data was collected with a seeing monitor made up of two components: a Solar Differential Image Motion Monitor (S-DIMM) and an array of six scintillometers known as the Shadow Band Ranger (SHABAR). The S-DIMM measures the total value of r_o integrated from the observing height to the top of the atmosphere. The SHABAR measures the steady and fluctuating intensity of sunlight in six detectors. It is used to estimate *Cn2(h)* and hence r_o as a function of height above the 8-m height at which the seeing monitor entrance aperture is mounted. The ATST seeing data obtained includes the time stamp of the measurement, the solar zenith angle, r_o at 8 and 28 meters, respectively and the surface winds and temperature. The ATST seeing data is collected during the daytime only and is valid between solar zenith angles of 5˚ and 85˚. Comparisons to the WRF simulations using the ATST data are therefore restricted to daytime. Figure 6 shows a comparison between WRF seeing and those obtained from the ATST dataset. Since the ATST data is referenced to the solar elevation angle of the sun the WRF data is referenced the same way to facilitate comparisons. Overall the WRF simulations agree best with the 8 meter ATST measurements, although WRF tends to underestimate the smallest values as well as the very largest. The WRF simulations agree very closely with the 28 meter estimates up to 4 cm but underestimate the larger values of r_o. We are unsure of the quality of the ATST measurements at very low sun angles. At these times the ATST data produces the largest r_o which would explain the discrepancies shown in Figure 6. Overall we believe the comparisons to be reasonable.

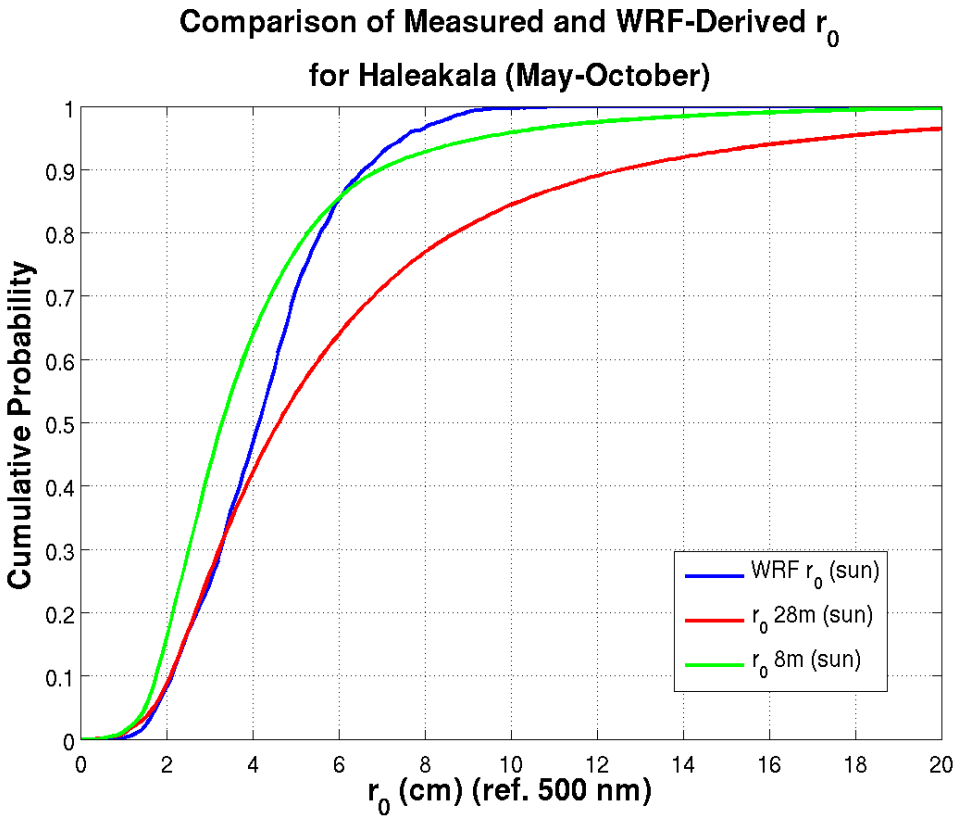

Figure 6. The cumulative distribution function (CDF) of r_o between WRF and ATST data. Data is referenced to zenith and is valid at 500 nm.

4. Summary and Conclusions

Simulations of OT were performed using the WRF model over the Hawaiian islands. Although the WRF model is incapable of simulating the very smallest values of r_o, it is capable of generally describing the climatology of the region of interest. This makes the model very convenient to use over areas where observations are not possible. The model did not simulate the so called neutral event which has been described in the literature. The model does an excellent job simulating the diurnal variation found in turbulence. Comparisons to the ATST data showed similar distributions although WRF was unable to simulate the large r_o observed at sunrise and sunset.

5. Acknowledgments

The authors thank the Maui High Performance Computing Center and the Northrop Grumman IS HPC center for providing simulation time on their clusters. The authors would also like to thank folks from the ATST program for supplying the SDIMM and SHABAR data which was collected at Haleakala and used in this analysis.

References

ATST Site Survey Working Group Final Report, 2004: http://atst.nso.edu/files/docs/RPT-0021.pdf

Bradley, E.S., L.C. Roberts, L. W. Bradford, M. Skinner, D.A. Nahrstedt, M.F. Waterson and J.R. Kuhn, 2006: Characterization of Meteorological and Seeing Conditions at Haleakala. *Publications of the Astronomical Soc. of the Pacific*, **118:**172-182.

Deardorff, J. W., 1980: Stratocumulus-capped mixed layers derived from a three-dimensional model. *Bound.-Layer Meteor.*, **18**, 495–527.

Fried, D. L., 1965: Statistics of a geometric representation of wavefront distortion. *J. Opt. Soc. Amer.*, **55**, 1427–1435.

Gerrity, J. P., T. L. Black, and R. E. Treadon, 1994: The numerical solution of the Mellor-Yamada level 2.5 turbulent kinetic energy equation in the Eta model. *Mon. Wea. Rev.*, **122**, 1640–1646.

Kondo, J., O. Kanechika, and N. Yasuda, 1978: Heat and momentum transfers under strong stability in the atmospheric surface layer. *J. Atmos. Sci.*, **35**, 1012–1021.

Mellor, G. L., and T. Yamada, 1982: Development of a turbulence closure model for geophysical fluid problems. *Rev. Geophys. Space Phys.*, **20**, 851–875.

Skamarock, W. C., J. B. Klemp, J. Dudhia, D. O. Gill, D. M. Barker, M. G. Duda, X.-Y. Huang, W. Wang, and J. G. Powers, 2008: A description of the advanced research WRF version 3. NCAR Technical Note, NCAR/TN-475+STR, 113 pp.

Tatarskii, V. I., 1971: The effects of the turbulent atmosphere on wave propagation. Technical Report, U.S. Department of Commerce, NTIS TT-68-50464, 472 pp.

Walters, D. L., and D. K. Miller, 1999: Evolution of an upper-tropospheric turbulence event—comparison of observations to numerical simulations. *Preprints, 13th Symposium on Boundary Layer Turbulence*, AMS, 157–160, Dallas, TX.